

LETTER • OPEN ACCESS

## Branchfall dominates annual carbon flux across lowland Amazonian forests

To cite this article: David C Marvin and Gregory P Asner 2016 *Environ. Res. Lett.* **11** 094027

View the [article online](#) for updates and enhancements.

You may also like

- [Current and future patterns of fire-induced forest degradation in Amazonia](#)  
Bruno L De Faria, Paulo M Brando, Marcia N Macedo et al.
- [Benchmarking carbon fluxes of the ISIMIP2a biome models](#)  
Jinfeng Chang, Philippe Ciais, Xuhui Wang et al.
- [The influence patterns of carbon flux in different climatic zones in China —Based on the complex network approach](#)  
Ting Qing, Fan Wang, Ruijin Du et al.

## Breath Biopsy Conference

5th & 6th November  
Online

Join the conference to explore the **latest challenges** and advances in **breath research**, you could even **present your latest work!**

**Register now for free!**

BREATH  
BIOPSY



Main talks

Early career sessions

Posters

## Environmental Research Letters



## LETTER

## OPEN ACCESS

## RECEIVED

19 February 2016

## REVISED

26 July 2016

## ACCEPTED FOR PUBLICATION

16 August 2016

## PUBLISHED

22 September 2016

Original content from this work may be used under the terms of the [Creative Commons Attribution 3.0 licence](#).

Any further distribution of this work must maintain attribution to the author(s) and the title of the work, journal citation and DOI.



## Branchfall dominates annual carbon flux across lowland Amazonian forests

David C Marvin and Gregory P Asner

Department of Global Ecology, Carnegie Institution for Science, 260 Panama St., Stanford, CA 94305, USA

E-mail: [gpa@carnegiescience.edu](mailto:gpa@carnegiescience.edu)**Keywords:** Amazon basin, Carnegie Airborne Observatory, forest carbon, gap dynamics, tropical forestSupplementary material for this article is available [online](#)

## Abstract

Tropical forests play an important role in the global carbon cycle, but knowledge of interannual variation in the total tropical carbon flux and constituent carbon pools is highly uncertain. One such pool, branchfall, is an ecologically important dynamic with links to nutrient cycling, forest productivity, and drought. Identifying and quantifying branchfall over large areas would reveal the role of branchfall in carbon and nutrient cycling. Using data from repeat airborne light detection and ranging campaigns across a wide array of lowland Amazonian forest landscapes totaling nearly 100 000 ha, we find that upper canopy gaps—driven by branchfall—are pervasive features of every landscape studied, and are seven times more frequent than full tree mortality. Moreover, branchfall comprises a major carbon source on a landscape basis, exceeding that of tree mortality by 21%. On a per hectare basis, branchfall and tree mortality result in 0.65 and 0.72 Mg C ha<sup>-1</sup> yr<sup>-1</sup> gross source of carbon to the atmosphere, respectively. Reducing uncertainties in annual gross rates of tropical forest carbon flux, for example by incorporating large-scale branchfall dynamics, is crucial for effective policies that foster conservation and restoration of tropical forests. Additionally, large-scale branchfall mapping offers ecologists a new dimension of disturbance monitoring and potential new insights into ecosystem structure and function.

## Introduction

Tropical forests play an important role in constraining atmospheric CO<sub>2</sub> concentrations. As the largest terrestrial carbon sink in the world, tropical forests are estimated to trap and store more than  $1.19 \pm 0.41$  Pg carbon per year—equivalent to the annual emissions of the European Union (Boden *et al* 2010)—that would otherwise remain in the atmosphere as heat-trapping CO<sub>2</sub> (Pan *et al* 2011). While ecologists are gaining ever-improving global information on tropical forest carbon stocks (Baccini *et al* 2012, Avitabile *et al* 2016), sub-continental estimates are still highly uncertain (Baccini and Asner 2013, Mitchard *et al* 2013, Sexton *et al* 2015). Accurately estimating changes over time in tropical forest aboveground carbon stocks (or carbon density, aboveground carbon density (ACD)) at sub-continental scales is crucial for

understanding the ecological and functional roles of these forests in a global context.

While carbon emissions resulting from tropical deforestation are better resolved (Harris *et al* 2012), carbon fluxes from intact forests are just as important but remain poorly understood. Multiple studies report a net carbon sink in the tropics based on evidence from repeated censuses of forest plots, remote sensing observations, atmospheric inverse modeling, and eddy flux towers (table S1). However, all of these estimates are highly uncertain and subject to considerable debate (Chambers *et al* 2009, 2013, Gloor *et al* 2012). Current estimates range from marginal sink values near zero to substantial sink values of up to 0.94 Mg C ha<sup>-1</sup> yr<sup>-1</sup>, with some reporting a carbon source in individual years. There are myriad causes for the high uncertainty surrounding estimates of ACD fluxes (Marvin *et al* 2014), but a fundamental source of this

uncertainty stems from the lack of large-scale, high-spatial resolution multi-temporal data.

Although rarely quantified, branchfall is an important ecological process that, when measured, can improve estimates of ecosystem processes. Tree crowns in tropical forests comprise approximately one-quarter to one-half of the total aboveground woody biomass (e.g., Higuchi *et al* 1998, Malhi *et al* 1999, Goodman *et al* 2014). As these crowns fragment over time they form an important biogeochemical flux, returning both carbon and nutrients to the soil beyond the standard flux from leaf litterfall or whole tree mortality. While branchfall and partial crown failures (i.e., non-fatal tree damage) are not generally considered a meaningful part of gap dynamics, they are sometimes measured as part of plot necromass surveys (e.g., Palace *et al* 2008, Doughty *et al* 2015, Malhi *et al* 2015), and are assumed to be implicitly captured over long time scales as a result of standard allometric scaling techniques. The ability to explicitly quantify and map branchfall (and tree mortality) over large areas will allow more accurate estimates of ecosystem carbon and nutrient flux by reducing uncertainties related to tree allometry and mortality (Palace *et al* 2008) and spatial upscaling from field plots/transects (Chambers *et al* 2013, Marvin *et al* 2014).

Understanding changes in branchfall and structural damage over time also provides ecologically important insights. Drought and other climate events (van der Meer and Bongers 1996, Doughty *et al* 2015), disease/pests, and mechanical stress from lianas and epiphytes (Putz 1984) are a few mechanisms that affect the rate of branchfall and other non-fatal tree damage. The resulting necromass produced by branchfall and tree mortality, as well as the increased light availability, creates structural habitat for a variety of organisms (e.g., Schemske and Brokaw 1981, Svenning 2000, Mac Nally *et al* 2001). Moreover, branchfall plays an important role in forest productivity (Chambers *et al* 2001), seedling/sapling regeneration and growth (Denslow 1987, Clark and Clark 1991), and nutrient cycling (Vitousek and Sanford 1986). A lack of branchfall data restricts the ability of ecologists to better understand and predict many ecosystem processes.

Here we examine 12 widely distributed landscapes totaling nearly 100 000 ha of lowland western Amazonian forest from a repeat airborne light detection and ranging (LiDAR) campaign (figure 1(A); table S2). We quantify full tree mortality (full canopy gaps, figure 1(D)), branch- and partial crownfall (upper canopy gaps, figure 1(E)) at 2 m spatial resolution, and calculate the estimated gross carbon source to the atmosphere of each gap type at 1 ha spatial resolution. No study has explicitly measured and incorporated branchfall as part of aboveground gross carbon losses at the landscape scale ( $10^3$ – $10^5$  ha), due to the difficulty of quantifying branchfall using field surveys

(Clark *et al* 2001a). We emphasize our measurement of gross rather than net carbon flux, with gross flux estimates (and gap formation rates generally) more pertinent to full accounting of tropical forest carbon dynamics. This study (1) investigates the difference between branchfall and tree mortality in western Amazon landscapes, (2) uncovers regional variation in gap dynamics, and (3) explores the potential for high-resolution measurement of gap dynamics to improve estimates of ecosystem processes.

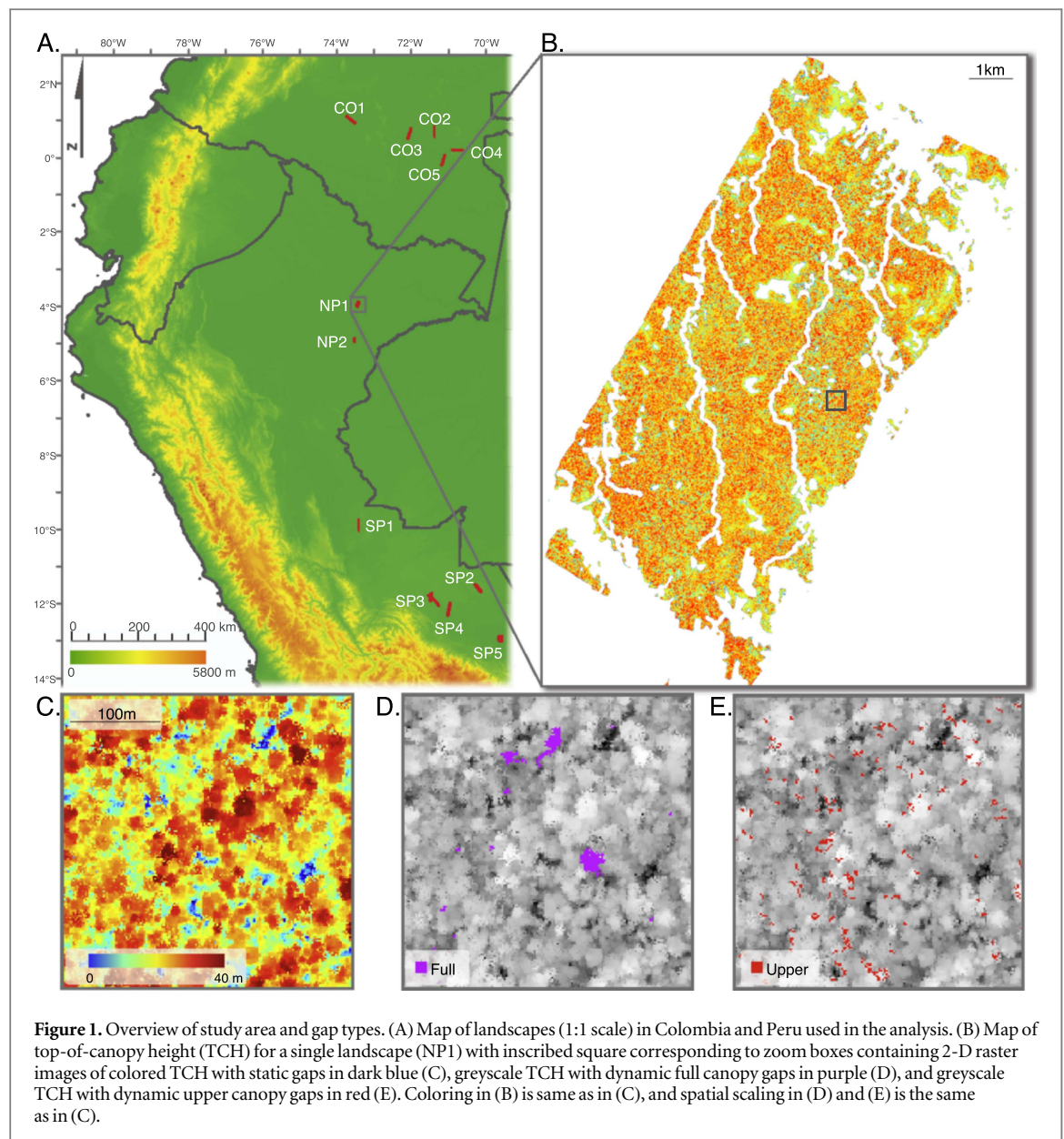
## Methods

### Study landscapes

We selected 12 landscapes distributed across a 1600 km longitudinal gradient of lowland tropical forests from northwest to southwest Amazonia (figure 1(A); table S2). Across all the landscapes, elevations ranged from 135 to 402 m above sea level (2 m resolution LiDAR digital terrain model (DTM), see below), mean annual precipitation (Huffman *et al* 2007) ranged from 1951 to 3492 mm (~25 km resolution), and mean annual temperature (Hijmans *et al* 2005) ranged from 24.3 to 26.7 °C (~5 km resolution). The geology of the landscapes is erosional *terra firme* substrate on elevated terraces, depositional floodplain substrate in low-lying areas near rivers and streams, or a mix of both. Dominant soil types (FAO-UNESCO 2005) in each landscape were Oxisols and Ultisols. These landscapes were chosen to be outside the main areas of the 2010 Amazon basin drought. The 2010 drought extended into the central Peruvian Amazon but was not extensive enough to affect the chosen landscapes mostly in the far SW and NE areas of Peru (Lewis *et al* 2011, Saatchi *et al* 2013). For each landscape we calculated mean dry-season (July–September) standardized precipitation evapotranspiration index (SPEI) (Vicente Serrano *et al* 2010) values extracted from SPEIbase (Begueria *et al* 2010) (table S2). None of the landscapes have a 2010 SPEI value below  $-1$ , which is considered to be the threshold for drought (Mitchell *et al* 2014).

### Airborne LiDAR collection and processing

Depending on the landscape, LiDAR data were either collected in 2011 and 2012, or 2011 and 2013 (table S2) using the Carnegie Airborne Observatory-2 (CAO) Airborne Taxonomic Mapping System (AToMS), which is carried onboard a Dornier 228 aircraft (Asner *et al* 2012). The AToMS LiDAR is a dual laser, scanning waveform system capable of operating at 500 000 laser shots per second. For the data collection, the aircraft was operated at speeds of up to 110 knots at an altitude averaging 2000 m above ground level. The LiDAR settings were maintained to sample a mean on-the-ground laser spot spacing of 2 shots  $m^{-2}$ , peaking at 4 shots  $m^{-2}$  in areas of flightline overlap. This level of sampling ensured that the derived LiDAR



measurements were highly precise in horizontal and vertical space (Asner *et al* 2012), with a combined between-flight uncertainty for top-of-canopy returns of  $\pm 17.0$  cm horizontally and  $\pm 15.6$  cm vertically for these flights.

Following data acquisition, laser ranges from the LiDAR were combined with embedded high resolution Global Positioning System-Inertial Measurement Unit data to determine the 3D locations of laser returns, producing a ‘cloud’ of LiDAR data (figure 2). A DTM, digital surface model, and top-of-canopy height (TCH) layer were produced for each landscape and for each year. We masked out non-forested areas, water bodies, and other anomalous landscape features. Each resulting landscape has at least 1900 ha of sampling area, with a total sampled area of 97 780 ha. See SI methods for more detail on the airborne LiDAR collection and processing.

### Canopy gap determination

Traditionally studies of gap dynamics employ the gap definition developed by Brokaw (1982), or a slight modification thereof, who defined a canopy gap as an opening ‘in the forest canopy extending through all levels down to an average height of two m above ground’. We find this definition to be overly simplistic and unfit for landscape-scale studies of gap dynamics using LiDAR-derived TCH data. Instead we define gaps based on the difference in relative height from the surrounding canopy. For each TCH layer, we created a  $TCH_{mean}$  layer using a mean smoothing filter with a one ha kernel. The  $TCH_{mean}$  was subtracted from the original TCH layer, and divided by  $TCH_{mean}$  to produce a relative TCH layer. For all classified gap types (see below) we computed the gap size-frequency variable  $\lambda$  for static full, dynamic full, and dynamic upper canopy gaps. We used the approach and R syntax provided by Asner *et al* (2013) and described in



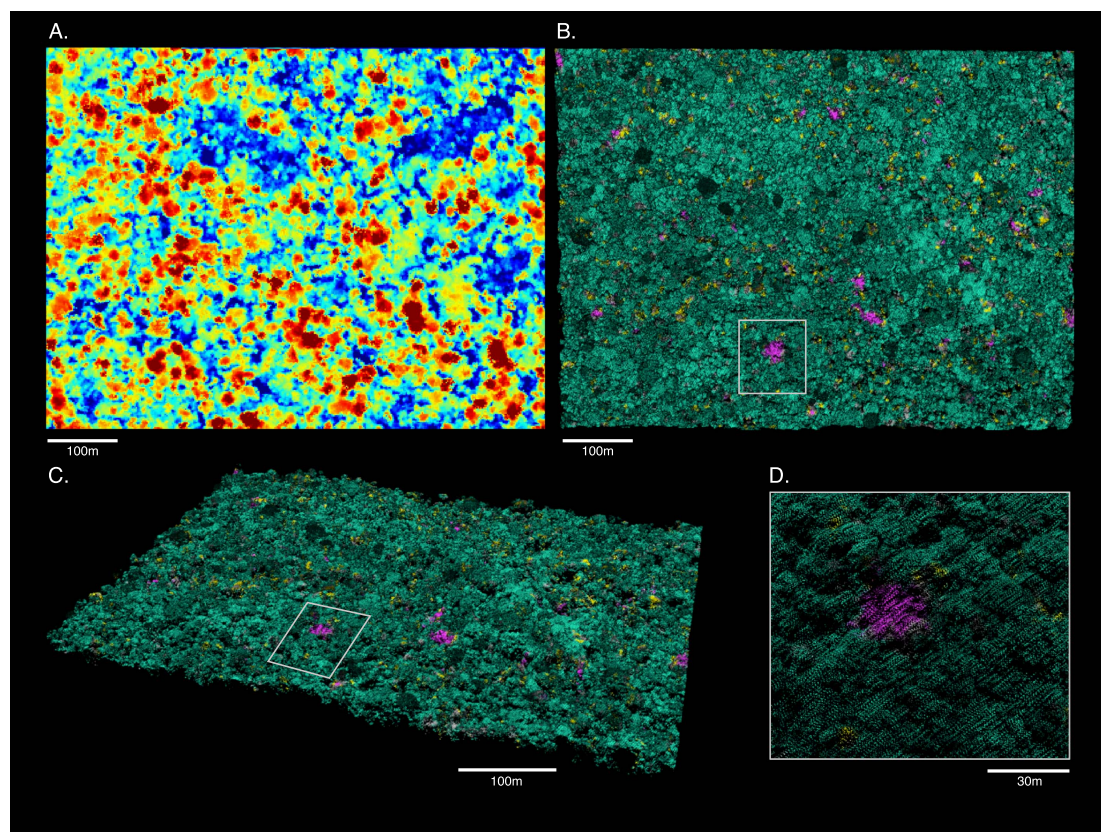


**Figure 2.** LiDAR 3-D point cloud from example area in landscape NP1 showing dynamic gaps. (A) LiDAR derived top-of-canopy height map at 2 m resolution with coloring as in Fig. 1C. (B) Top view of LiDAR three-dimensional point cloud with full (purple) and upper (yellow) canopy gaps, and (C) isometric view of (B). (D) Zoom inset from (B) and (C) showing an isometric view of a large full canopy and multiple smaller upper canopy gaps. In (B-D) the green colored points are year 2 data, while gap colored points (purple and yellow) are points that were present in year 1 but were not present in year 2. Gray points are those present in year 1 no longer present in year 2 but did not meet the dynamic gap criterion (see Methods).

more detail by Marvin *et al* (2014). We calculated the gap density (gaps  $\text{ha}^{-1}$ ) and the mean gap size per unit area for all gap types.

#### Static and dynamic full canopy gaps

Static gaps (those present only at a single time period) were classified as having a relative TCH of  $-0.7$  to  $-1.0$ , or 70%–100% below the mean forest height of the surrounding 1 ha at each data collection time period. This allows identification of gaps over short timescales (1–2 years) using airborne LiDAR even when tree fall debris, understory shrubs or small trees, and/or rapidly growing pioneer species fill in the full canopy gap above the 2 m Brokaw threshold. Other thresholds considered yielded similar results (Asner *et al* 2013).

Using the final static gap layers from the two sampling years, we classified dynamic full gaps (those newly formed during the sampling period) as only those pixels that were not classified as a static gap in Year 1, but met the static gap definition above in Year 2. To reduce gap false positives, only three or more contiguous pixels (areas  $\geq 12 \text{ m}^2$ ) were retained as static or dynamic full canopy gaps.

#### Dynamic upper canopy gaps

We refine and extend the concept of upper canopy gaps to be applicable to dynamic measurements of forest gaps. Dynamic upper canopy gaps are newly formed gaps during the sampling period resulting from medium-to-large branch falls and partial crown failures of trees that form the canopy layer of an intact forest. These gaps are isolated to the canopy layer and do not extend to the ground. For each landscape, Year 1 TCH was subtracted from Year 2 TCH, and divided by Year 1 TCH to produce the relative TCH change between the two sampling periods. We define dynamic upper canopy gaps as a relative loss in canopy height between the two sampling periods of 0.1–0.4, or a 10%–40% height loss below the mean forest height of the surrounding 1 ha. This percentage range was chosen to be equivalent to the full gap canopy definition while remaining isolated to only the upper canopy. Using a range of relative TCH change (as opposed to a static length) allows flexibility in identifying upper canopy gaps formed in anomalously short and tall trees. We then filtered the data and only retained areas as dynamic upper canopy gaps that were (a)  $\geq 90\%$  of the mean forest height (from the one ha mean smoothing filter) in Year 1 and (b) composed of

three or more contiguous pixels. The 90% threshold isolates the analysis to only the uppermost parts of the canopy, and the three pixel minimum grouping reduces the possibility that horizontal shifts in the canopy between the two sampling periods (due to wind, growth, or LiDAR co-alignment errors) could result in upper canopy gap false positives. We conservatively chose the 10% threshold as an upper bound because this begins to approach the LiDAR vertical error of  $\pm 15$  cm in the case of shorter stature trees. Although we have high confidence that the LiDAR sampling density was high enough to accurately sample true 'TCH', an analysis of whether deciduous vegetation leads to false-positive gap classifications found that it did not (see SI discussion). Other studies have utilized analyses of single-pixel changes between two LiDAR time periods with data from an even earlier model of the CAO LiDAR that was used in the current study (Kellner *et al* 2011, Kellner and Asner 2014). We are far more conservative in this analysis by limiting gap detection to only groups of three or more contiguous pixels that have dropped in height far outside the LiDAR limits of uncertainty.

#### Allometric and ACD calculations

We calculate ACD at one-hectare resolution using a plot-aggregate allometric approach, parameterized with stem data from 166 western Amazon field inventory plots (Asner and Mascaro 2014). Full and upper canopy ACD layers were created separately using different parameterizations of the plot-aggregate allometry. For the full canopy ACD layer we used the LiDAR-derived plot mean TCH from the western Amazon plot network, and field-based BA,  $\rho_{BA}$ , and ACD. For the upper canopy ACD layer (ACD<sub>crown</sub>) we used data from direct biomass harvests (Nogueira *et al* 2008, Goodman *et al* 2014) that reported the percent total ACD contained by the crown. The percentage of carbon contained in the crowns of the harvested tree dataset was used to convert plot ACD to plot ACD<sub>crown</sub> using a simulation that propagates the uncertainty in tree crown dataset (see SI methods for details).

We produced 'gap-corrected' ACD layers by creating a map of height loss only within full or upper canopy gaps at 2 m resolution, subtracting this from the Year 1 TCH layer, resampling to one-hectare resolution, and applying the same models and parameterizations as the initial ACD layer or ACD<sub>crown</sub>. Residual uncertainties from the ACD models were propagated through to each gap-corrected ACD layer. These gap-corrected layers isolate the effect of gaps on ACD by holding forest growth to zero. By subtracting these layers from their associated initial ACD layers, we derive the amount of carbon lost due to each type of canopy gap.

Carbon loss ratios were calculated by bootstrapping ACD values from each landscape for each

gap type and calculating the ratio of upper to full gap carbon loss. We performed this 5000 times for each landscape, and used the mean and 2.5% and 97.5% quantiles for the confidence interval. The uncertainty in the sub-regional (NW and SW Amazon) and total western Amazon regional carbon loss values were calculated by summing the variance of each landscape value, dividing by the number of landscapes, and multiplying by 1.96 to obtain the 95% confidence intervals. See SI methods for more details on the allometric calculations and assumptions, and the ACD and flux calculations.

## Results

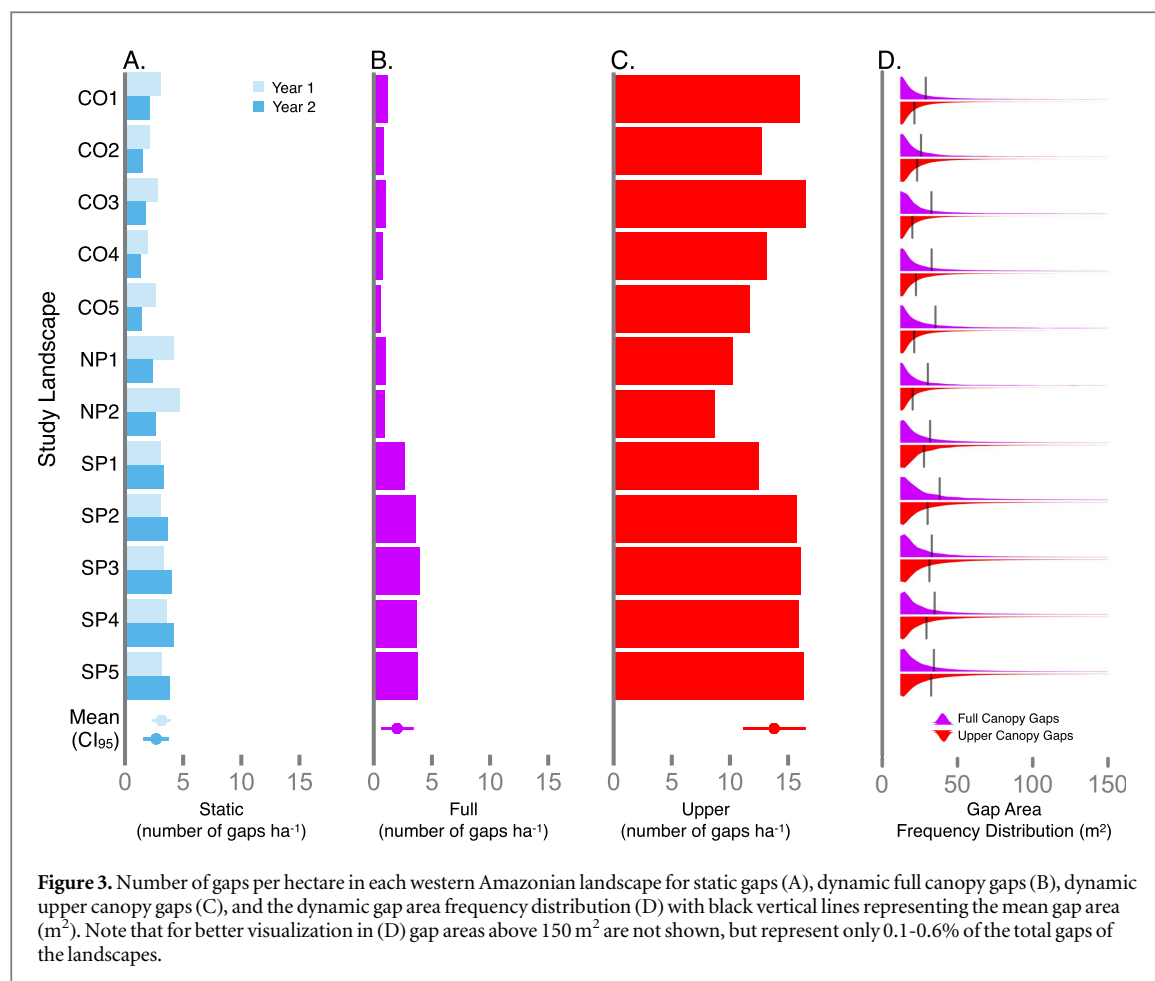
### Branchfall dynamics

In the absence of major drought-related tree mortality and damage, we find that upper canopy gaps (branchfall) are far more frequent and pervasive than full canopy gaps (tree mortality) across all western Amazonian landscapes studied. While each upper canopy gap on average contains 32% of the LiDAR-measured volume and 13% of the carbon compared to an average full canopy gap, they are almost 700% as frequent (figure 3, table 1). Moreover, at the hectare-scale branchfall consistently occurs across at least 99.7% of every landscape, while full tree mortality is more heterogeneously distributed, covering anywhere from 41.9% to 99.4% of the landscape (figure 4(A)).

This disparity in both frequency and distribution results in branchfall exerting an unexpectedly large influence on the carbon dynamics of the western Amazon: on a landscape basis branchfall represents 21% more gross carbon loss than full tree mortality (figure 4(B)). This is calculated from the average ratio of total landscape upper canopy gap carbon loss to the total landscape full canopy gap carbon loss, providing a large-scale context of the influence of each gap type on the carbon cycle. Alternatively, we calculate a per hectare branchfall gross source of 0.65 (95% confidence interval [CI<sub>95</sub>, 0.60–0.70]) Mg C ha<sup>-1</sup> yr<sup>-1</sup> to the atmosphere across lowland western Amazonian forests, with full tree mortality resulting in a 0.72 (CI<sub>95</sub> 0.67–0.76) Mg C ha<sup>-1</sup> yr<sup>-1</sup> gross source (table 2).

### Regional variation

In the forests of the SW Amazon, upper canopy gaps are a substantial portion (ca 60%–80%; figure 4(B), table 2) of the total gross landscape carbon loss to the atmosphere, primarily due to their larger size relative to upper canopy gaps in the NW (figure 2, table 1). In contrast, relative to full canopy gaps upper canopy gaps in NW Amazon forests are a proportionally larger carbon loss (ca 100%–240%; figure 4(B), table 2), but smaller absolute carbon loss. More importantly, the decrease in upper gap absolute gross carbon loss as you move from the SW to the NW is small (ca 80%) compared to the decrease in full gap absolute gross



carbon loss (ca 300%). Branchfall remains remarkably consistent among landscapes across the western Amazon region compared to full tree mortality.

## Discussion

Our analysis of the dynamics of 2.7 million individual gaps across ca 100 000 ha of tropical forest reveals the critical role that branchfall plays in the carbon and nutrient cycles of the western Amazon. The discovery that branchfall is far more frequent and pervasive than full tree mortality, resulting in the release of 21% more gross carbon at the landscape-scale, has numerous implications for understanding the ecology of the region. The methods developed here allow spatially explicit monitoring of branchfall and full tree mortality across landscapes at high resolution. Branchfall carbon losses have not previously been mapped and calculated over such large scales, nevertheless our findings are consistent with, although less variable than, field plot-based gross carbon loss estimates of branchfall and tree damage (0.1–3.2 Mg C ha<sup>-1</sup> yr<sup>-1</sup>) (e.g., Chambers *et al* 2001, Clark *et al* 2001b, Chave *et al* 2003, Palace *et al* 2008, Chao *et al* 2009).

The stark contrast that we identify between the forests of the NW and SW Amazon (figure 4, table 2) expresses underlying differences in soil fertility,

geology, precipitation, and diversification rates that all affect the floristic composition, wood density, carbon stocks, and natural disturbance regimes of the two sub-regions (Gentry 1988, Phillips *et al* 2004, Quesada *et al* 2012, Baker *et al* 2014). Relative to the NW Amazon, forests in the SW Amazon are characterized by lower wood density, lower ACD, and faster tree turnover all resulting from higher soil nutrients and stronger seasonality. We find that while the carbon loss from full tree mortality decreases substantially between the SW and NW, branchfall carbon loss decreases only slightly (figure 4). This has major implications for the central/eastern Amazon basin, which has a two-fold decrease in the estimated rate of tree turnover compared to the western Amazon (Phillips *et al* 2004). Our results suggest that regardless of tree turnover rate, branchfall exerts a substantial influence on forest carbon dynamics and nutrient cycling across the entire Amazon basin.

The heterogeneous distribution of full gap frequency both within and among landscapes (figure 4(A)) found by this study highlights the risk of scaling field-based estimates of carbon flux to landscapes or regions (see Marvin *et al* 2014). A recent simulation study of central Amazon gap dynamics (Chambers *et al* 2013) found ca 9%–17% of tree mortality events over time are missed by single hectare

**Table 1.** Summary of gap results.

| Landscape             | Region   | Size (ha) | Static Year 1      |                        |               | Static Year 2      |                        |               | Dynamic Full       |                        |                       |               | Dynamic Upper      |                        |                       |               |
|-----------------------|----------|-----------|--------------------|------------------------|---------------|--------------------|------------------------|---------------|--------------------|------------------------|-----------------------|---------------|--------------------|------------------------|-----------------------|---------------|
|                       |          |           | # ha <sup>-1</sup> | area (m <sup>2</sup> ) | gap $\lambda$ | # ha <sup>-1</sup> | area (m <sup>2</sup> ) | gap $\lambda$ | # ha <sup>-1</sup> | area (m <sup>2</sup> ) | vol (m <sup>3</sup> ) | gap $\lambda$ | # ha <sup>-1</sup> | area (m <sup>2</sup> ) | vol (m <sup>3</sup> ) | gap $\lambda$ |
| CO1                   | Colombia | 10 438    | 3.1                | 40.5                   | 1.41          | 2.1                | 40.1                   | 1.41          | 1.2                | 32.8                   | 480                   | 1.45          | 16.0               | 21.9                   | 123                   | 1.49          |
| CO2                   | Colombia | 3815      | 2.1                | 36.6                   | 1.42          | 1.5                | 33.6                   | 1.43          | 1.0                | 25.8                   | 370                   | 1.47          | 16.5               | 22.6                   | 136                   | 1.48          |
| CO3                   | Colombia | 9494      | 2.8                | 40.0                   | 1.41          | 1.7                | 36.9                   | 1.42          | 0.9                | 28.9                   | 400                   | 1.46          | 12.7               | 20.5                   | 119                   | 1.50          |
| CO4                   | Colombia | 4740      | 2.0                | 41.4                   | 1.42          | 1.4                | 41.7                   | 1.42          | 0.8                | 25.4                   | 364                   | 1.48          | 13.2               | 18.2                   | 108                   | 1.51          |
| CO5                   | Colombia | 8517      | 2.6                | 37.5                   | 1.42          | 1.4                | 38.4                   | 1.42          | 0.6                | 32.7                   | 488                   | 1.46          | 11.7               | 19.2                   | 108                   | 1.51          |
| NP1                   | N. Peru  | 6157      | 4.1                | 43.9                   | 1.40          | 2.4                | 40.5                   | 1.41          | 1.0                | 35.4                   | 485                   | 1.43          | 10.2               | 20.1                   | 123                   | 1.50          |
| NP2                   | N. Peru  | 1966      | 4.6                | 52.2                   | 1.39          | 2.6                | 42.3                   | 1.41          | 1.0                | 30.3                   | 429                   | 1.46          | 8.7                | 19.3                   | 123                   | 1.51          |
| <b>NW Amazon mean</b> |          |           | <b>3.0</b>         | <b>41.7</b>            | <b>1.41</b>   | <b>1.9</b>         | <b>39.1</b>            | <b>1.42</b>   | <b>0.9</b>         | <b>30.2</b>            | <b>431</b>            | <b>1.46</b>   | <b>12.7</b>        | <b>20.3</b>            | <b>120</b>            | <b>1.50</b>   |
| SP1                   | S. Peru  | 6039      | 3.1                | 53.2                   | 1.40          | 3.3                | 44.5                   | 1.41          | 2.6                | 31.8                   | 424                   | 1.44          | 12.5               | 26.8                   | 179                   | 1.46          |
| SP2                   | S. Peru  | 10 631    | 3.1                | 54.0                   | 1.38          | 3.7                | 59.3                   | 1.38          | 3.6                | 38.2                   | 462                   | 1.42          | 15.8               | 28.8                   | 173                   | 1.44          |
| SP3                   | S. Peru  | 15 229    | 3.3                | 57.1                   | 1.38          | 4.0                | 55.3                   | 1.39          | 3.9                | 32.9                   | 426                   | 1.44          | 16.1               | 30.0                   | 182                   | 1.44          |
| SP4                   | S. Peru  | 10 161    | 3.6                | 57.2                   | 1.38          | 4.2                | 52.8                   | 1.39          | 3.7                | 34.8                   | 468                   | 1.44          | 15.9               | 27.6                   | 166                   | 1.45          |
| SP5                   | S. Peru  | 10 592    | 3.1                | 53.1                   | 1.39          | 3.9                | 57.4                   | 1.39          | 3.8                | 34.3                   | 432                   | 1.44          | 16.3               | 30.4                   | 157                   | 1.43          |
| <b>SW Amazon mean</b> |          |           | <b>3.2</b>         | <b>54.9</b>            | <b>1.39</b>   | <b>3.8</b>         | <b>53.9</b>            | <b>1.39</b>   | <b>3.5</b>         | <b>34.4</b>            | <b>442</b>            | <b>1.46</b>   | <b>15.3</b>        | <b>28.7</b>            | <b>171</b>            | <b>1.49</b>   |
| <b>Total</b>          |          |           | <b>3.1</b>         | <b>47.2</b>            | <b>1.40</b>   | <b>2.7</b>         | <b>45.2</b>            | <b>1.41</b>   | <b>2.0</b>         | <b>31.9</b>            | <b>436</b>            | <b>1.45</b>   | <b>13.8</b>        | <b>23.8</b>            | <b>141</b>            | <b>1.48</b>   |

Vol (m<sup>3</sup>) is the LiDAR-measured volume loss from each gap type (area x mean TCH loss per gap). Gap  $\lambda$  is the gap size-frequency scaling parameter (see Methods), with values <2 indicating that large gaps are more dominant than small gaps. SW Amazon landscapes have a two year repeat flight interval, but have been converted to annual rates.



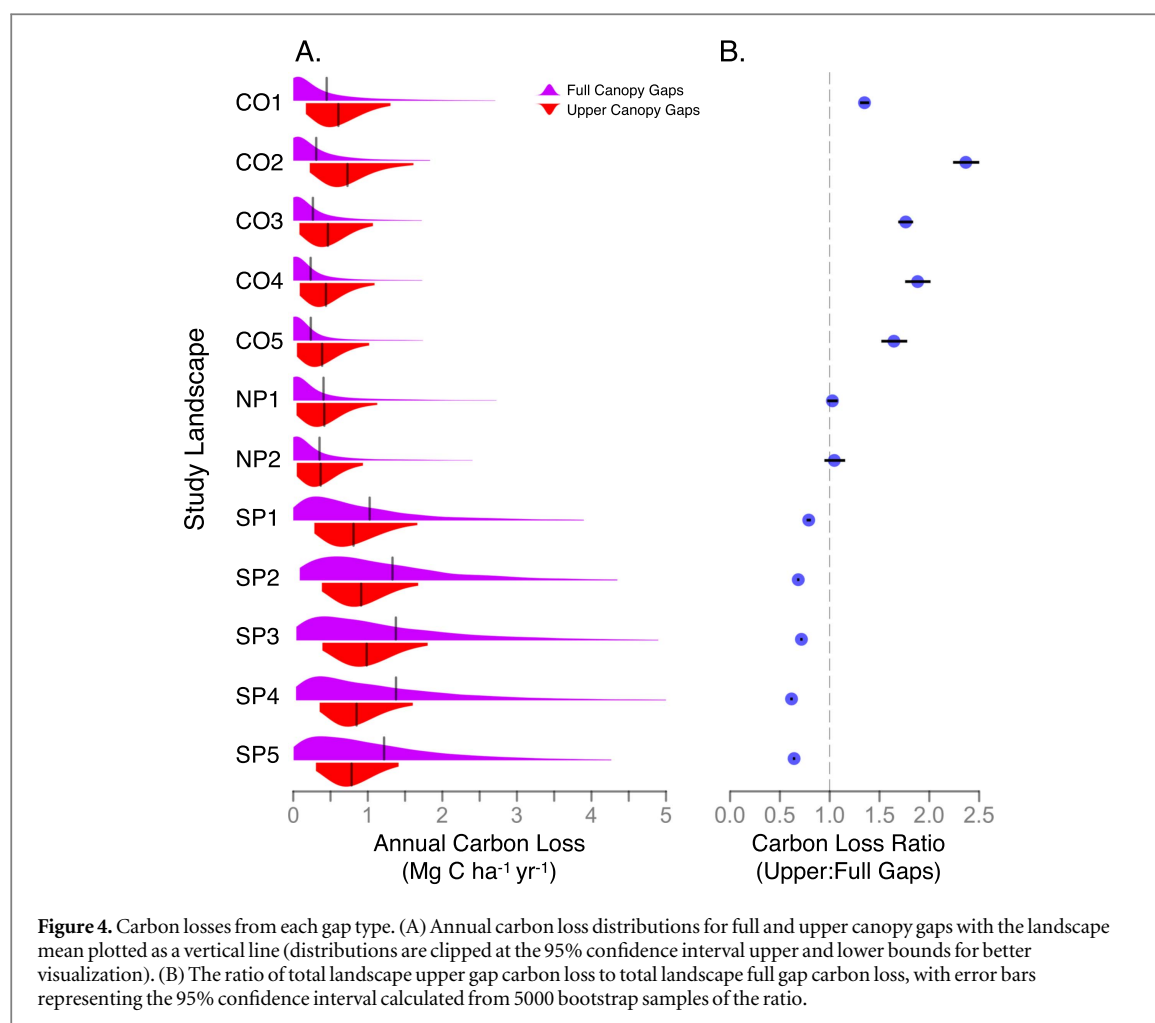


**Table 2.** Summary of carbon results

| Landscape             | Region   | Size (ha) | Total ACD <sup>a</sup><br>(MgC ha <sup>-1</sup> ) | Crown ACD <sup>a</sup><br>(MgC ha <sup>-1</sup> ) | ACD Loss (MgC ha <sup>-1</sup> ) |             |             |             |             |             |
|-----------------------|----------|-----------|---|---|----------------------------------|-------------|-------------|-------------|-------------|-------------|
|                       |          |           |   |   | Full Gaps                        |             |             | Upper Gaps  |             |             |
|                       |          |           |   |   | Mean                             | CI–         | CI+         | Mean        | CI–         | CI+         |
| CO1                   | Colombia | 10 438    | 106.8   | 47.3  | 0.45                             | 0.21        | 0.69        | 0.61        | 0.37        | 0.84        |
| CO2                   | Colombia | 3815      | 125.5   | 55.0  | 0.31                             | –0.14       | 0.76        | 0.73        | 0.28        | 1.18        |
| CO3                   | Colombia | 9494      | 108.8   | 48.1  | 0.26                             | 0.01        | 0.51        | 0.47        | 0.21        | 0.72        |
| CO4                   | Colombia | 4740      | 116.5   | 51.3  | 0.23                             | –0.16       | 0.62        | 0.44        | 0.05        | 0.83        |
| CO5                   | Colombia | 8517      | 111.5   | 49.3  | 0.24                             | –0.03       | 0.51        | 0.39        | 0.11        | 0.66        |
| NP1                   | N. Peru  | 6157      | 107.1   | 48.5  | 0.41                             | 0.12        | 0.70        | 0.42        | 0.10        | 0.73        |
| NP2                   | N. Peru  | 1966      | 119.7   | 53.6  | 0.35                             | –0.26       | 0.96        | 0.37        | –0.25       | 0.99        |
| <b>NW Amazon mean</b> |          |           | <b>113.7</b>                                      | <b>50.4</b>                                       | <b>0.32</b>                      | <b>0.25</b> | <b>0.39</b> | <b>0.49</b> | <b>0.41</b> | <b>0.57</b> |
| SP1                   | S. Peru  | 6039      | 122.3   | 54.8  | 1.03                             | 0.85        | 1.21        | 0.81        | 0.63        | 0.99        |
| SP2                   | S. Peru  | 10 631    | 99.1  | 45.6  | 1.33                             | 1.23        | 1.43        | 0.91        | 0.80        | 1.02        |
| SP3                   | S. Peru  | 15 229    | 100.4   | 46.0  | 1.38                             | 1.28        | 1.48        | 0.99        | 0.89        | 1.08        |
| SP4                   | S. Peru  | 10 161    | 92.0  | 42.6  | 1.38                             | 1.28        | 1.48        | 0.85        | 0.74        | 0.96        |
| SP5                   | S. Peru  | 10 592    | 81.7  | 38.3  | 1.22                             | 1.14        | 1.30        | 0.78        | 0.69        | 0.88        |
| <b>SW Amazon mean</b> |          |           | <b>99.1</b>                                       | <b>45.5</b>                                       | <b>1.27</b>                      | <b>1.26</b> | <b>1.28</b> | <b>0.87</b> | <b>0.86</b> | <b>0.88</b> |
| <b>Total</b>          |          |           | <b>107.6</b>                                      | <b>48.4</b>                                       | <b>0.72</b>                      | <b>0.67</b> | <b>0.76</b> | <b>0.65</b> | <b>0.60</b> | <b>0.70</b> |

<sup>a</sup> Calculated from forested areas with average height  $\geq 16$  m (see Methods)

Confidence intervals are mean  $\pm$  SD\*1.96. SD includes the propagated model and spatial uncertainty. Sub-regional and regional means and CIs are calculated from the landscape means with propagated uncertainty. SW Amazon landscapes have a two year repeat flight interval, but have been converted to annual rates.

plots due to the temporal heterogeneity in large multi-tree deaths. Moreover, field-based estimates of carbon flux may need to be corrected for branchfall carbon losses depending on the methodology underlying the specific allometric scaling equation that is employed. Whether or not undamaged trees (i.e. no missing branches or partial crowns) were harvested and weighed to parameterize the allometric equation determines if a branchfall correction is needed (see Chambers *et al* 2001 for an in-depth discussion of this issue). These potential sources of error require further investigation by the forest carbon research community.

There are limitations to this study that must be considered in the context of branchfall detection and carbon loss. Not all trees that die immediately form a full canopy gap, and similarly some branchfall events may originate from these standing dead trees. Trees with low wood density may have a higher rate of branch breakage (but may also more easily snap at trunk level), and trees with higher wood density may uproot easier. Both of these factors would underestimate carbon losses from full tree mortality and overestimate carbon losses from branchfall. On the other hand, branchfall and partial crown failure events that leave an opening extending down (or close) to the forest floor would be counted as a full canopy gap, having the opposite effect on carbon loss partitioning. There is also a lack of data on the partitioning of crown and trunk biomass in harvested trees. We used the only published datasets from Amazonia that separately reported crown and trunk biomass to parameterize our crown ACD allometric equation. It is unknown whether this dataset is representative of the true distribution of crown carbon, and could result in either an over- or underestimation of branchfall carbon loss by this study. Finally, further study is needed before airborne LiDAR can be utilized for estimates of short-term forest growth and subsequent estimates of net forest carbon flux, rather than the gross carbon source from gaps described here.

## Conclusion

Considerable uncertainty in the ecosystem processes of tropical forests remains (e.g., Schimel *et al* 2015), with substantial repercussions for the understanding and prediction of the global climate system (Bodman *et al* 2013). Our finding that gross carbon losses from branchfall on average exceed that of full tree mortality reveals the importance of large-scale, high-resolution measurements of tropical forests in space and time. Reducing the uncertainty of one variable in the carbon balance equation (in this case, gross carbon loss from tree mortality and damage) will lead to better estimates of yearly net carbon flux. The power of forest carbon monetization policies (such as REDD+) to mitigate climate change—through increased forest

conservation and restoration—ultimately relies on our ability to precisely estimate carbon flux. Reduced uncertainty should lead to lower carbon market volatility and higher economic benefits for countries and landowners (Newell and Stavins 2000, Köhl *et al* 2009).

More broadly, our results demonstrate that the dynamics of intact Amazon forests are heterogeneous, further highlighting the need for spatially resolved tropical carbon and nutrient fluxes at sub-continental scales. Such data can be combined with targeted field surveys to increase the accuracy of net carbon flux, decomposition, and nutrient cycling estimates. Dynamic global vegetation models (DGVMs) need better representation of these ecosystem processes within forested biomes (Moorcroft 2006, Medlyn *et al* 2015). Estimates of these processes can be input to forest individual-based models that can be used to improve DGVMs (Purves and Pacala 2008, Shugart *et al* 2015). To achieve these goals, there is a crucial need for (a) vastly improved spatial and temporal field-based measurements of carbon and nutrient cycle components, and (b) pantropical airborne LiDAR sampling able to resolve landscape carbon heterogeneity and the subtle but important fluxes of carbon from tree damage. Both avenues of research can jointly work to shrink the level of uncertainty in tropical forest ecosystem processes, resulting in increased predictive accuracy and climate-change mitigation efficacy.

The ability to map individual branchfalls, in addition to full tree mortality, across landscapes over time provides ecologists with a new dimension of disturbance monitoring. Monitoring branchfall may reveal subtle and immediate ecosystem responses as these damage mechanisms may not be sufficient for, or result in delayed, full-tree mortality. Both the causes and consequences of ecosystem-level branchfall can then be assessed. The methods developed here to identify and quantify branchfall at landscape scales can provide new insight into ecosystem structure and functioning.

## Acknowledgments

We thank N Vaughn and C Anderson for assistance with processing the LiDAR data and the gap carbon calculations. J Kellner provided comments to improve the manuscript. This study was supported by the John D and Catherine T MacArthur Foundation. The Carnegie Airborne Observatory is made possible by the Gordon and Betty Moore Foundation, the John D and Catherine T MacArthur Foundation, Avatar Alliance Foundation, W M Keck Foundation, the Margaret A Cargill Foundation, Grantham Foundation for the Protection of the Environment, Mary Anne Nyburg Baker and G Leonard Baker Jr, and William R Hearst III.

## References

- Asner G P, Kellner J R, Kennedy-Bowdoin T, Knapp D E, Anderson C and Martin R E 2013 Forest canopy gap distributions in the southern Peruvian Amazon *PLoS One* **8** e60875
- Asner G P, Knapp D E, Boardman J, Green R O, Kennedy-Bowdoin T, Eastwood M, Martin R E, Anderson C B and Field C B 2012 Carnegie Airborne Observatory-2: increasing science data dimensionality via high-fidelity multi-sensor fusion *Remote Sens. Environ.* **124** 454–65
- Asner G P and Mascaro J 2014 Mapping tropical forest carbon: calibrating plot estimates to a simple LiDAR metric *Remote Sens. Environ.* **140** 614–24
- Avitabile V *et al* 2016 An integrated pan-tropical biomass map using multiple reference datasets *Glob. Change Biol.* **22** 1406–20
- Baccini A and Asner G P 2013 Improving pantropical forest carbon maps with airborne LiDAR sampling *Carbon Manage.* **4** 591–600
- Baccini A *et al* 2012 Estimated carbon dioxide emissions from tropical deforestation improved by carbon-density maps *Nat. Clim. Change* **2** 182–5
- Baker T R *et al* 2014 Fast demographic traits promote high diversification rates of Amazonian trees *Ecol. Lett.* **17** 527–36
- Beguieria S, Vicente Serrano S M and Angulo-Martínez M 2010 A multiscale global drought dataset: the SPEIbase: a new gridded product for the analysis of drought variability and impacts *Bull. Am. Meteorol. Soc.* **91** 1351–6
- Boden T A, Marland G and Andres R J 2010 Global, regional, and national fossil-fuel CO<sub>2</sub> emissions CDIAC ([http://cdiac.ornl.gov/trends/emis/overview\\_2010.html](http://cdiac.ornl.gov/trends/emis/overview_2010.html))
- Bodman R W, Rayner P J and Karoly D J 2013 Uncertainty in temperature projections reduced using carbon cycle and climate observations *Nat. Clim. Change* **3** 725–9
- Brokaw N 1982 The definition of treefall gap and its effect on measures of forest dynamics *Biotropica* **14** 158–60
- Chambers J Q, Negron-Juarez R I, Hurtt G C, Marra D M and Higuchi N 2009 Lack of intermediate-scale disturbance data prevents robust extrapolation of plot-level tree mortality rates for old-growth tropical forests *Ecol. Lett.* **12** E22–5
- Chambers J Q, Negron-Juarez R I, Marra D M, Di Vittorio A, Tews J, Roberts D, Ribeiro G H P M, Trumbore S E and Higuchi N 2013 The steady-state mosaic of disturbance and succession across an old-growth Central Amazon forest landscape *Proc. Natl Acad. Sci. USA* **110** 3949–54
- Chambers J Q, Santos Dos J, Ribeiro R J and Higuchi N 2001 Tree damage, allometric relationships, and above-ground net primary production in central Amazon forest *Forest Ecol. Manage.* **152** 73–84
- Chao K J, Phillips O L, Baker T R, Peacock J, Lopez Gonzalez G, Vasquez Martinez R, Monteagudo A and Torres Lezama A 2009 After trees die: quantities and determinants of necromass across Amazonia *Biogeosciences* **6** 1615–26
- Chave J, Condit R, Lao S, Caspersen J, Foster R and Hubbell S 2003 Spatial and temporal variation of biomass in a tropical forest: results from a large census plot in Panama *J. Ecol.* **91** 240–52
- Clark D A, Brown S, Kicklighter D W, Chambers J Q, Thomlinson J R and Ni J 2001a Measuring net primary production in forests: concepts and field methods *Ecol. Appl.* **11** 356–70
- Clark D A, Brown S, Kicklighter D W, Chambers J Q, Thomlinson J R, Ni J and Holland E A 2001b Net primary production in tropical forests: an evaluation and synthesis of existing field data *Ecol. Appl.* **11** 371–84
- Clark D B and Clark D A 1991 The impact of physical damage on canopy tree regeneration in tropical rain forest *J. Ecol.* **79** 447
- Denslow J S 1987 Tropical rainforest gaps and tree species diversity *Annu. Rev. Ecol. Syst.* **18** 431–51
- Doughty C E *et al* 2015 Drought impact on forest carbon dynamics and fluxes in Amazonia *Nature* **519** 78–82
- FAO-UNESCO 2005 *Soil Map of the World* (Washington, DC: USDA-NRCS, Soil Science Division, World Soil Resources)
- Gentry A H 1988 Changes in plant community diversity and floristic composition on environmental and geographical gradients *Ann. Mo. Bot. Gard.* **75** 1–34
- Gloor M *et al* 2012 The carbon balance of South America: a review of the status, decadal trends and main determinants *Biogeosciences* **9** 5407–30
- Goodman R C, Phillips O L and Baker T R 2014 The importance of crown dimensions to improve tropical tree biomass estimates *Ecol. Appl.* **24** 680–98
- Harris N L, Brown S, Hagen S, Baccini A and Houghton R A 2012 *Progress Toward a Consensus on Carbon Emissions From Tropical Deforestation: Policy Brief* (Washington, DC: Meridian Inst)
- Higuchi N, Santos Dos J, Ribeiro R J, Minette L and Biot Y 1998 Aboveground biomass of the Brazilian Amazon rainforest *Acta Amazonica* **28** 153–66
- Hijmans R J, Cameron S E, Parra J L, Jones P G and Jarvis A 2005 Very high resolution interpolated climate surfaces for global land areas *Int. J. Climatol.* **25** 1965–78
- Huffman G J, Alder R F, Bolvin D T, Gu G, Nelkin E J, Bowman K P, Hong Y, Stocker E F and Wolff D 2007 The TRMM multisatellite precipitation analysis (TMPA): quasi-global, multiyear, combined-sensor precipitation estimates at fine scales *J. Hydrometeorol.* **8** 38–55
- Kellner J R and Asner G P 2014 Winners and losers in the competition for space in tropical forest canopies *Ecol. Lett.* **17** 556–62
- Kellner J R, Asner G P, Vitousek P M, Twitten M A, Hotchkiss S and Chadwick O A 2011 Dependence of forest structure and dynamics on substrate age and ecosystem development *Ecosystems* **14** 1156–67
- Köhl M, Baldauf T, Plugge D and Krug J 2009 Reduced emissions from deforestation and forest degradation (REDD): a climate change mitigation strategy on a critical track *Carbon Balance Manage.* **4** 10
- Lewis S L, Brando P M, Phillips O L, van der Heijden G M F and Nepstad D 2011 The 2010 Amazon Drought *Science* **331** 554–554
- Mac Nally R, Parkinson A, Horrocks G, Conole L and Tzaros C 2001 Relationships between terrestrial vertebrate diversity, abundance and availability of coarse woody debris on south-eastern Australian floodplains *Biol. Conservation* **99** 191–205
- Malhi Y, Baldocchi D D and Jarvis P G 1999 The carbon balance of tropical, temperate and boreal forests *Plant Cell Environ.* **22** 715–40
- Malhi Y *et al* 2015 The linkages between photosynthesis, productivity, growth and biomass in lowland Amazonian forests *Glob. Change Biol.* **21** 2283–95
- Marvin D C, Asner G P, Knapp D E, Anderson C B, Martin R E, Sinca F and Tupayachi R 2014 Amazonian landscapes and the bias in field studies of forest structure and biomass *Proc. Natl Acad. Sci. USA* **111** E5224–32
- Medlyn B E *et al* 2015 Using ecosystem experiments to improve vegetation models *Nat. Clim. Change* **5** 528–34
- Mitchard E, Saatchi S S, Baccini A, Asner G P, Goetz S J, Harris N L and Brown S 2013 Uncertainty in the spatial distribution of tropical forest biomass: a comparison of pan-tropical maps *Carbon Balance Manage.* **8** 10
- Mitchell P J, O'Grady A P, Hayes K R and Pinkard E A 2014 Exposure of trees to drought-induced die-off is defined by a common climatic threshold across different vegetation types *Ecol. Evol.* **4** 1088–101
- Moorcroft P R 2006 How close are we to a predictive science of the biosphere? *Trends Ecol. Evol.* **21** 400–7
- Newell R G and Stavins R N 2000 Climate change and forest sinks: factors affecting the costs of carbon sequestration *J. Environ. Educ.* **40** 211–35
- Nogueira E M, Fearnside P M, Nelson B W, Barbosa R I and Hermanus Keizer E W 2008 Estimates of forest biomass in the Brazilian Amazon: new allometric equations and adjustments to biomass from wood-volume inventories *Forest Ecol. Manage.* **256** 1853–67

- Palace M, Keller M and Silva H 2008 Necromass production: studies in undisturbed and logged Amazon forests *Ecol. Appl.* **18** 873–84
- Pan Y *et al* 2011 A large and persistent carbon sink in the world's forests *Science* **333** 988–93
- Phillips O L, Baker T, Arroyo L and Higuchi N 2004 Pattern and process in Amazon tree turnover, 1976–2001 *Phil. Trans. R Soc. B* **359** 381–407
- Purves D and Pacala S 2008 Predictive models of forest dynamics *Science* **320** 1452–3
- Putz F E 1984 The natural history of lianas on Barro Colorado Island, Panama *Ecology* **65** 1713–24
- Quesada C A *et al* 2012 Basin-wide variations in Amazon forest structure and function are mediated by both soils and climate *Biogeosciences* **9** 2203–46
- Saatchi S, Asefi-Najafabady S, Malhi Y, Aragão L E O C, Anderson L O, Myneni R B and Nemani R 2013 Persistent effects of a severe drought on Amazonian forest canopy *Proc. Natl Acad. Sci. USA* **110** 565–70
- Schemske D W and Brokaw N 1981 Treefalls and the distribution of understory birds in a tropical forest *Ecology* **62** 938
- Schimel D, Stephens B B and Fisher J B 2015 Effect of increasing CO<sub>2</sub> on the terrestrial carbon cycle *Proc. Natl Acad. Sci. USA* **112** 436–41
- Sexton J O *et al* 2015 Conservation policy and the measurement of forests *Nat. Clim. Change* **6** 192–6
- Shugart H H, Asner G P, Fischer R and Huth A 2015 Computer and remote-sensing infrastructure to enhance large-scale testing of individual-based forest models *Front. Ecol. Environ.* **13** 503–11
- Svenning J-C 2000 Small canopy gaps influence plant distributions in the rain forest understory *Biotropica* **32** 252–61
- van der Meer P J and Bongers F 1996 Patterns of tree-fall and branch-fall in a tropical rain forest in French Guiana *J. Ecol.* **84** 19–29
- Vicente Serrano S M, Beguería S and López-Moreno J I 2010 A multiscalar drought index sensitive to global warming: the standardized precipitation evapotranspiration index *J. Clim.* **23** 1696–718
- Vitousek P M and Sanford R L 1986 Nutrient cycling in moist tropical forest *Annu. Rev. Ecol. Syst.* **17** 137–67